ORIGINAL ARTICLE

Induction of rapid, reproducible hepatic ablations using next-generation, high frequency irreversible electroporation (H-FIRE) *in vivo*

Imran A. Siddiqui[1], Eduardo L. Latouche[2], Matthew R. DeWitt[2], Jacob H. Swet[1], Russell C. Kirks[1], Erin H. Baker[1], David A. Iannitti[1], Dionisios Vrochides[1], Rafael V. Davalos[2] & Iain H. McKillop[1]

[1]Division of HPB Surgery, Dept. Surgery, Carolinas Medical Center, Charlotte, NC, and [2]School of Biomedical Engineering and Mechanics, Virginia Polytechnic and State University, Blacksburg, VA

Abstract

Introduction: Irreversible electroporation (IRE) offers an alternative to thermal tissue ablation *in situ*. High-frequency IRE (H-FIRE), employing ultra-short bipolar electrical pulses, may overcome limitations associated with existing IRE technology to create rapid, reproducible liver ablations *in vivo*.

Methods: IRE electrodes (1.5 cm spacing) were inserted into the hepatic parenchyma of swine (n = 3) under surgical anesthesia. In the absence of paralytics or cardiac synchronization five independent H-FIRE ablations were performed per liver using 100, 200, or 300 pulses (2250 V, 2-5-2 μs configuration). Animals were maintained under isoflurane anesthesia for 6 h prior to analysis of ablation size, reproducibility, and apoptotic cell death.

Results: Mean ablation time was 230 ± 31 s and no EKG abnormalities occurred during H-FIRE. In 1/15 HFIRE's minor muscle twitch (rectus abdominis) was recorded. Necropsy revealed reproducible ablation areas (34 ± 4 mm^2, 88 ± 11 mm^2 and 110 ± 11 mm^2; 100-, 200- and 300-pulses respectively). Tissue damage was predominantly apoptotic at pulse delivery $\leq$200 pulses, after which increasing evidence of tissue necrosis was observed.

Conclusion: H-FIRE can be used to induce rapid, predictable ablations in hepatic tissue without the need for intraoperative paralytics or cardiac synchronization. These advantages may overcome limitations that restrict currently available IRE technology for hepatic ablations.

Received 1 April 2016; accepted 23 June 2016

Correspondence

Iain H. Mckillop, Department of Surgery, Carolinas Medical Center, Charlotte, NC, 28203, USA.
Tel: +1 (704) 355 2846. Fax: +1 (704) 355 7202. E-mail: Iain.Mckillop@carolinashealthcare.org

Introduction

Thermal tissue destruction using radiofrequency or microwave ablation (RFA/MWA) is an effective treatment for primary and metastatic liver tumors.[1–3] Using RFA or MWA tissue within the ablation zone is thermally destroyed, resulting in necrotic tissue death and preservation of surrounding liver tissue.[3,4] For tumors >3 cm, a radiologic response rate of 91% following RFA is reported with rates of local recurrence, distant intrahepatic recurrence, and extrahepatic metastasis, independent of tumor size.[5] Increasing evidence suggests MWA offers superior physical properties for tumor ablation compared to RFA,[2] and reproducible large-volume hepatic ablations (3–7 cm) can be effectively performed with MWA.[6] In addition, MWA creates more predictable ablations in the (relative) absence of heat sink, while allowing real-time, intraoperative ablation visualization with color Doppler ultrasound (US).[7]

Irreversible electroporation (IRE) is an alternative to thermal ablation that employs high-voltage (1–3 kV) short (50–100 μs) monopolar pulses (Fig. 1a). Briefly, pulsatile electrical currents are discharged between 2 and 6 electrodes placed across the

Previous communications: Presented, in part, at the 12th World Congress of the International Hepato-Pancreato Biliary Association (IHPBA), Sao Paulo, Brazil (2016).

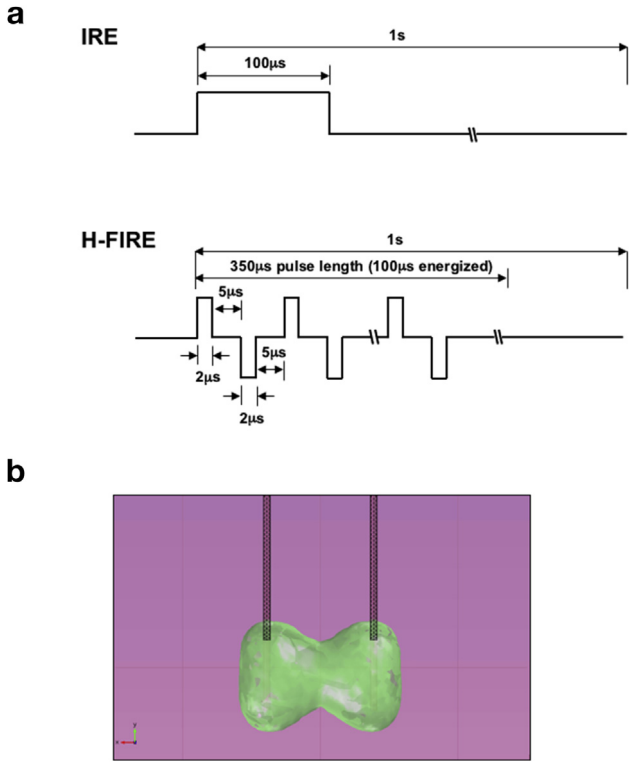

Figure 1 **Comparison between conventional irreversible electroporation (IRE) and high-frequency IRE (H-FIRE).** **a**). Schematic representation of electrical pulse delivery using conventional IRE (upper) and H-FIRE (lower). **b**). Theoretical, computer modeling of predicted ablation zone created using H-FIRE technology

target region, resulting in nanoscale pore formation in cell membranes located within electric fields ≥500 V/cm. Once these nanopores form, cells are unable to regulate ion and water movement leading to the induction of apoptosis.[8] Unlike thermal ablation, events following IRE occur in the absence of coagulative necrosis, and underlying organ architecture, including vascular and ductal structures, is preserved.[9,10] In addition, the (relative) absence of thermal damage using IRE means the ablation region is predominantly contained between the electrodes, the spacing of which can be varied, with spacing up to 4 cm being reported for dual electrodes.[10,11] Clinical outcomes of IRE in HPB surgery are reported, IRE being demonstrated to be a safe and effective means to ablate tissue.[10,12] With refinement of technique and improved patient selection, local complications (including bleeding, bile duct perforation, and bowel injury) can be minimized. A recent, multi-institutional series demonstrated safety and efficacy of IRE for treating pancreatic adenocarcinoma.[13]

Despite the potential advantages IRE offers over thermal ablation, other factors must be considered. For example, cardiac electrical asynchrony, with potential for arrhythmia, and severe tetanic muscle contraction[8,10] means IRE must be performed in conjunction with synchronization to cardiac activity and muscle paralysis. Similarly, the time required for electrode placement and synchronization of electrical pulses with cardiac output, means intraoperative time for IRE is typically longer than required for RFA/MWA,[2,3,8,13,14] the majority of which is performed using a laparoscopic approach.[2,6] Following IRE ablation the slower induction of apoptotic cell death, as opposed to rapid thermal necrosis using RFA/MWA, can limit post-operative imaging to determine extent of tumor destruction. Collectively, these factors have limited the use of IRE in HPB surgery to treating cancers for which resection or thermal ablation are unviable.[13]

High frequency irreversible electroporation (H-FIRE) is a novel IRE approach developed to overcome many of the challenges existing IRE faces.[15,16] Unlike the monopolar electrical pulses used in existing IRE (delivered in the 100 μs range), H-FIRE employs ultra-short (1–2 μs) bipolar electrical pulses (Fig. 1a).[15] By doing so, H-FIRE changes polarity rapidly enough to minimize nerve or muscle stimulation. Similar to IRE, changes in cellular transmembrane potential within the H-FIRE field result in nanopore formation and cellular apoptosis (Fig. 1b).[16] These properties allow H-FIRE to generate reproducible, homogenous tissue ablations in the absence of muscle contractions, so obviating the requirement of intraoperative paralytics and, potentially, cardiac synchronization.[15,17] Thus, H-FIRE should require shorter ablation times than existing IRE, while maintaining the advantage of preserving the underlying architecture.

This study sought to determine whether H-FIRE can be employed to induce reproducible, effective ablations in a swine liver model *in vivo*, and establish optimal pulse delivery parameters in the hepatic parenchyma to induce apoptotic cell death.

Methods

Assurances

Female Yorkshire pigs were used for these studies (Palmetto Research Swine, Reevesville, SC). All studies were approved by the Institutional Animal Care and Use Committee (IACUC) and conformed to the National Institutes of Health Guide for Animal Care and Use of Laboratory Animals.

Surgical procedures

In total, 15 ablations were performed in 3 separate animals with n = 5 ablations/H-FIRE pulse-setting. Prior to initiating studies animals were randomized for pulse delivery setting (100-, 200- or 300-pulses) such that no animal received more than 2 H-FIRE ablations at the same pulse setting. The number of ablations performed was selected to provide sufficient statistical power for analysis, while ensuring a sufficient distance existed between ablation sites to avoid prior ablations, and to reduce potential variability in time between completing all of the ablations in a single animal and euthanasia 6 h later.

Following premedication with atropine (0.04 mg/kg) anesthesia was induced using Telazol (5 mg/kg, i.m.), Xylazine (2 mg/kg, i.m.) and sodium thiopental (20 mg/kg, i.v.). Animals were intubated and surgical anesthesia maintained with isoflurane. Pre-emptive analgesia (morphine, 0.06 mg/kg, i.m.) was administered prior to commencing surgery. An accelerometer was placed on the electrode handles, and a Bovie cautery grounding pad placed on the thigh. Animals were continuously monitored using telemetry and pulse-oximetry.

The abdominal wall was prepared using a chlorhexidine solution (×2), an upper midline incision (15–20 cm) made, and a Balfour retractor placed to expose the liver. Ultrasound (US) guidance was used to identify major hepatic vessels. Two NanoKnife® IRE electrodes were positioned in parallel with spacing set to 1.5 cm, and the active portion of the electrodes exposed to a length of 1 cm. The electrodes were inserted into the hepatic parenchyma under US guidance to a final depth of 2.5–3.0 cm, with care taken to avoid major vascular and biliary

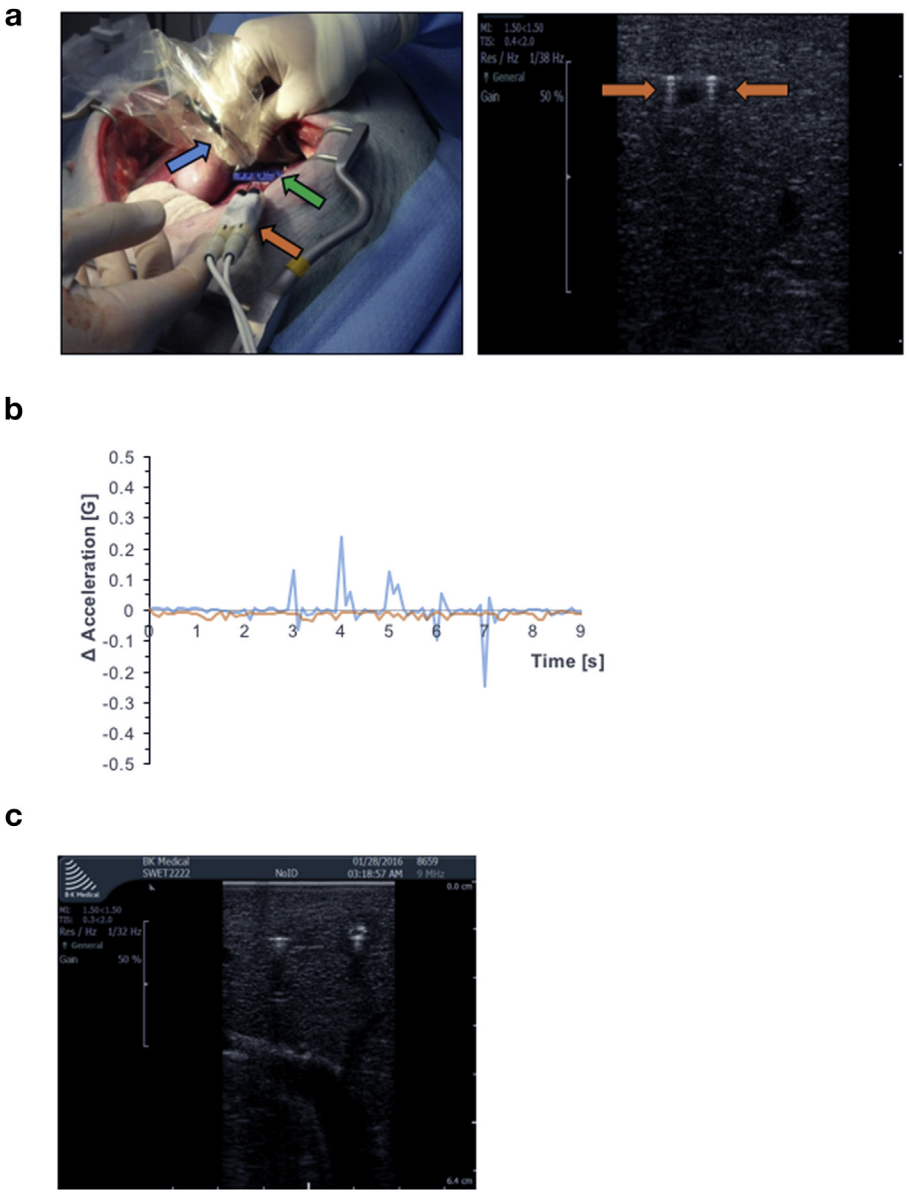

Figure 2 **Intraoperative images and data collection using high frequency irreversible electroporation (H-FIRE) to perform hepatic ablations**. **a**) Intraoperative image of H-FIRE electrode insertion in the hepatic parenchyma (➔ = US probe, ➔ = electrode spacer, ➔ = electrodes), and representative US image illustrating post-electrode insertion into hepatic parenchyma (➔ = electrodes). **b**) Representative accelerometer data illustrating minor twitching of abdominal muscle when electrodes placed within 5 cm of the hilum (blue line) *versus* no twitching (orange line). **c**) Representative intraoperative US images illustrating halo effect during ablation

structures during and after placement (Fig. 2a). Prior to pulse delivery care was taken to ensure no part of the electrode was in contact with the abdominal wall or retractor.

Using computerized algorithms and custom software 2 250 V was delivered. H-FIRE pulses had a total energized time of 100 μs, which consisted of 25 cycles of a 2-5-2 configuration (2 μs on, 5 μs off, 2 μs on). Pulses were delivered at a frequency of 1 burst/s in sets of 50-pulses, separated by a 10 s delay. Pulses were evaluated continuously by measuring changes in tissue resistance between the electrodes to determine whether changes in tissue resistance-conductivity or heterogeneity altered pulse delivery. Analysis of muscle twitching was provided *via* displacement signals from an accelerometer attached to the electrode. Animals were survived under isoflurane anesthesia with continuous monitoring of vital signs prior to being euthanized (12 ml EUTHASOL®) 6 h after the final ablation. The time point for euthanasia was based on time required for apoptotic (caspase 3) activity to be detected in tissue following H-FIRE and veterinary advice for maintaining animals under continuous anesthesia post-H-FIRE.

Necropsy

Following removal, the liver was inspected and sites of ablation photographed. The ablation site was grossly sectioned at 5–7 mm intervals in parallel with, and transversely to, the plane of electrode insertion. A 5 mm section in the center of the ablated region was evaluated and photographed, followed by placement in either triphenyltetrazolium chloride (TTC) solution (3 h, room temperature) or 10% neutral buffered formalin overnight (NBF, 4 °C).

Calculation of ablation area and volume

Triphenyltetrazolium chloride (TTC) is a redox indicator used as a marker of cellular respiration and has been reported to expose the area of IRE in liver tissue. Briefly, immersion of tissue in a 1% TTC solution allows metabolically active tissue to be discerned from inactive, dying tissue since the grey TTC compound is only reduced to (a bright red) 1,3,5-triphenylformazan compound in living cells.[12,18] In contrast, necrotic cells do not take up TTC and appear white. Total ablation area, apoptotic area, and necrotic area of tissue in sections cut in planes longitudinal and transverse to the angle of electrode insertion were used to calculate ablation areas and volumes.

Histological analysis and apoptotic (caspase 3) activity

Following tissue fixation, samples were prepared and sectioned (6–8 μm) for hematoxylin and eosin (H&E) staining as previously reported.[19] H&E stained slides were analyzed to confirm ablation areas and representative images captured. To analyze apoptotic cell death immunohistochemistry (IHC) was performed on sections using an antibody specific against cleaved caspase 3 (AbCam, Cambridge, MA).[20] Representative images of sections (n = 10/ablation) were taken and blind scored for cleaved caspase-3 expression using a scale of; 0 = No detectable staining 1= < 25% staining, 2 = 25–50% staining, 3 = 50–75% staining, 4= > 75% staining.

Statistical analysis

We used Kruskal–Wallis to test total ablation, apoptotic, and necrotic areas among the 4 pulse setting groups and Wilcoxon signed rank tests for the pairwise testing with no adjustment for multiple comparisons. We compared caspase scores across the 4 pulse groups using Skillings–Mack non-parametric procedure which accounts for the block design and replicates within blocks. We used the same procedure for testing between any two pulse groups with no adjustments for multiple comparisons. Analyses were conducted using SAS Enterprise Guide (V6.4) (Cary, NC). A p-value of <0.05 was considered significant.

Results

Intraoperative observations

All 3 experimental animals survived the H-FIRE procedures for the duration of the experimental protocol. Throughout the period of H-FIRE ablations no change in cardiac activity or blood-oxygen saturation were observed, independent of the H-FIRE setting employed (data not shown). In 1/15 H-FIREs (200 pulses, 4th ablation of 5 performed, ablation in the center of the right hepatic lobe) minor twitching of the rectus abdominis was measured (Fig. 2b). Despite twitching coinciding with pulse delivery, no changes in cardiac activity were noted for the duration of the ablation. During H-FIRE, signals were visualized as moving longitudinal interference signals using US and ablated areas were seen as a hyperechoic center surrounded by a hypoechoic rim (halo-effect) when compared to the surrounding parenchyma (isoechoic) (Fig. 2c), similar to that reported by other investigators using existing IRE technology (NanoKnife®).[21] In total 15 independent H-FIRE ablations were performed in 3 separate animals. The range for ablation times was 110–350 s (mean ablation time was 230 ± 31 s (n = 15)). Following H-FIRE the site of electrode insertion was clearly visible and the liver surface marked. Any bleeding following electrode removal was minimal, and ceased following application of gentle pressure with a sterile gauze pad.

Necropsy

Gross inspection of tissue following cross-section revealed an overall spherical-ellipsoid shaped ablation at lower pulse number (100 pulses) increasing, to a dumbbell-shaped ablation when ellipsoids converged at higher pulse delivery (300-pulses, Fig. 3a).

Following TTC staining, clear demarcation between apoptotic tissue (grey-white) and healthy, metabolically viable tissue (deep red) was visible (Fig. 3b). Immediately surrounding the tract of electrode insertion tissue staining was predominantly white, suggesting more severe necrotic damage due to the inability of cells undergoing necrotic cell death to take up TTC (Fig. 3b).

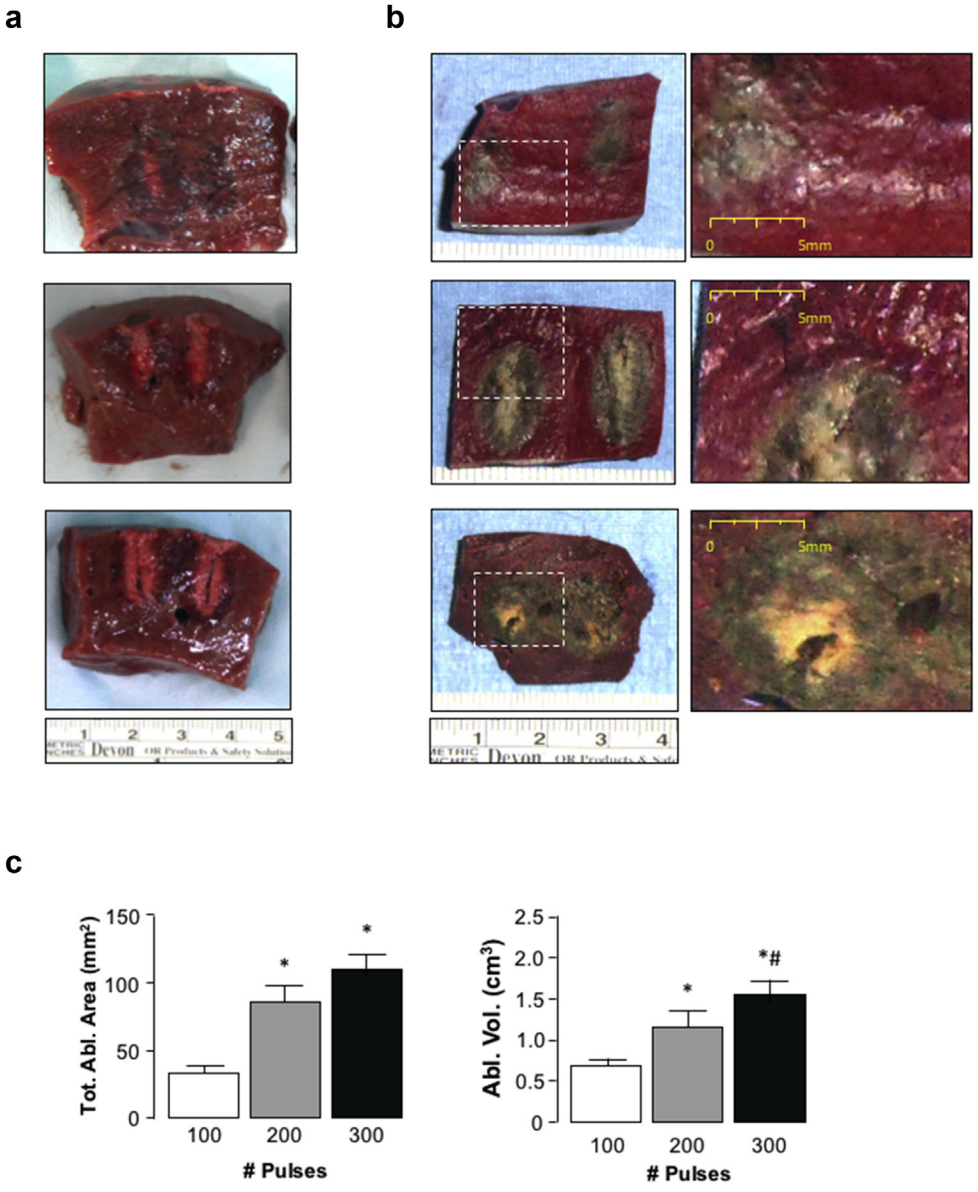

Figure 3 **Comparison of hepatic ablations using high frequency irreversible electroporation (H-FIRE) with varying pulse number delivery.** **a**) Representative gross pathology images illustrating longitudinal sections of ablation zones following 100-, 200- or 300-pulses (2 250 V, 2-5-2 pulse configuration, 1.5 cm spacing). **b**) Representative images of hepatic tissue following H-FIRE delivery at 100, 200 or 300-pulses (2250 V, 2-5-2 pulse configuration, 1.5 cm spacing) following TTC staining. **c**) Ablation area and ablation volume calculated following TTC staining. *p < 0.05 200- and 300-pulses *versus* 100-pulses, #p < 0.05 200- *versus* 300-pulses, n = 5

With increasing number of pulses increased necrotic damage was observed (Fig. 3b). Ablation measurement revealed significantly increasing ablation area with increasing pulse-number; at 100 pulses the median ablation area was 33 mm^2 (range 18–54 mm^2, mean 34 ± 4 mm^2); at 200 pulses the median ablation area was 76 mm^2 (range 64–122 mm^2, mean 88 ± 11 mm^2); at 300 pulses the median ablation area was 125 mm^2 (range 78–130 mm, mean 110 ± 11 mm^2) (Fig. 3c). Calculated ablation volumes were consistent with measurement of ablation area, 200- and 300-pulses leading to ablation volumes significantly greater than those achieved with 100-pulses, while ablation volumes using 300-pulses was significantly greater than those achieved with 200-pulses (Fig. 3c).

Analysis of areas of apoptotic cell death demonstrated increased apoptosis at increasing pulse delivery (Fig. 4a), 28 ± 3 mm^2 (median = 33 mm^2, range 16–46 mm^2) for 100-pulses, 64 ± 9 mm^2 (median = 68 mm^2, range 43–86 mm^2) for 200-pulses, and 80 ± 10 mm^2 (median = 88 mm^2, range

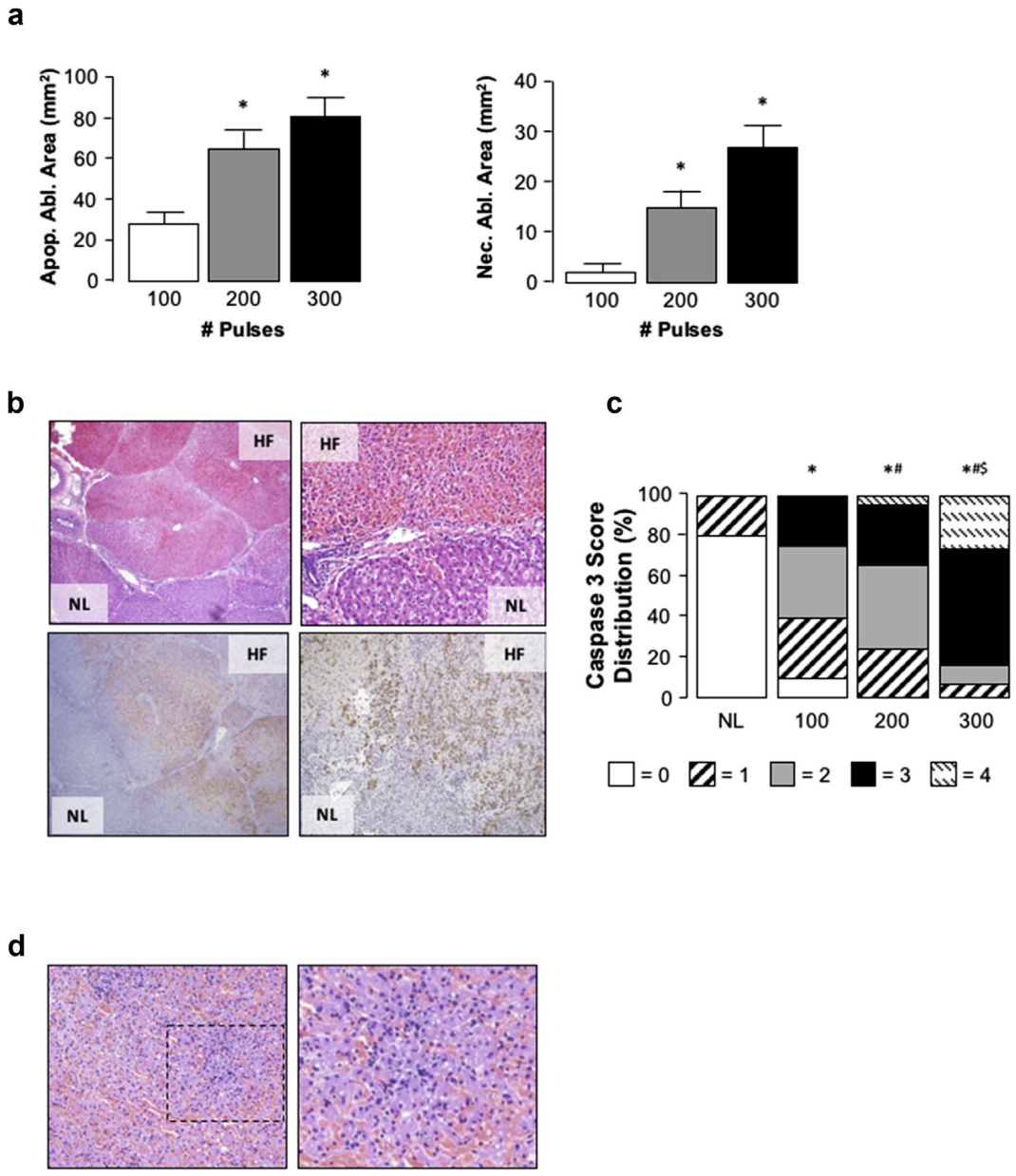

Figure 4 Analysis of cell death and tissue architecture in the liver following high frequency irreversible electroporation (H-FIRE). Apoptotic and necrotic tissue area calculated following TTC staining of tissue. *p < 0.05 200- and 300-pulses versus 100-pulses, n = 5. **b**) Representative H&E and immunohistochemistry staining using an anti-caspase-3 antibody illustrating region between H-FIRE (HF) and normal liver (NL) following 200-pulse H-FIRE delivery (2250 V, 2-5-2 pulse configuration, 1.5 cm spacing) (×40 and ×100). Caspase 3 activity/apoptosis stains brown. **c**) Blind scoring (score scale 0–4) of caspase-3 staining in liver tissue following 100-, 200- and 300-pulse delivery (2250 V, 2-5-2 pulse configuration, 1.5 cm spacing). *p < 0.05 *versus* normal tissue (no H-FIRE), $^{\#}$p < 0.05 200- and 300-pulses *versus* 100-pulses, $^{\$}$p < 0.05 200- *versus* 300-pulses. **d**) Representative image (×40 and ×100) highlighting immune cell infiltration in ablated regions following 300-pulse H-FIRE delivery (2250 V, 2-5-2 pulse configuration, 1.5 cm spacing)

51–106 mm^2) for 300-pulses, *p < 0.05 300- and 200-pulses *versus* 100-pulses, n = 5. Analysis of necrotic death revealed increasing necrosis with increasing pulse number (Fig. 4a, 2 ± 2 mm^2 (median = 0 mm^2, range 0–8 mm^2) for 100-pulses, 15 ± 4 mm^2 (median = 16 mm^2, range 4–27 mm^2) for 200-pulses, and 27 ± 5 mm^2 (median = 24 mm^2, range 18–44 mm^2) for 300-pulses, *p < 0.05 300- and 200-pulses *versus* 100-pulses, n = 5, p = 0.09 200- *versus* 300-pulses).

Histological analysis confirmed the area of hepatic ablation induced by H-FIRE was contained within regions between the two

H-FIRE electrodes, clear demarcation between ablated and non-ablated tissue being evident (Fig. 4b). Gross structural analysis revealed apparent preservation of hepatic architecture (including vascular and biliary structures) and lobular integrity/connective tissue (Fig. 4b). Immunohistochemistry using an antibody against cleaved caspase-3 mirrored histological data, with extensive caspase activity being detected in the ablated region (Fig. 4b). Blind scoring of cleaved caspase-3 confirmed these findings, significantly increased caspase score being associated with increasing pulse number (Fig. 4c). Finally, microscopic analysis of tissue demonstrated notable immune cell infiltration at the 300-pulse setting, an effect not observed at lesser pulse numbers (100- and 200-pulses) suggesting the potential of increased necrotic cell death at 300-pulse settings (Fig. 4d).

Discussion

A significant concern for all modes of tumor ablation is the risk of incomplete ablation and local recurrence.[6,22] In many instances RFA for hepatic ablations has been replaced by MWA because of increased predictability of thermal tissue destruction.[6,14,23] Nonetheless, the tendency toward "over-treatment" exists to ensure the lesion is destroyed.[6,22,23] With IRE, ablation is largely restricted to the area contained within the electrodes, with minimal collateral thermal damage.[8,12]

Using H-FIRE at lower pulse delivery settings (100- and 200-pulses), detectable ablations appeared restricted to the area immediately around the electrodes at necropsy. However, closer analysis of TTC staining and caspase-3 activity noted apoptosis in regions between the two electrodes using caspase 3 detection that was not immediately apparent using TTC. These data suggest that in these regions, while retaining sufficient metabolic activity to reduce TTC, apoptotic process were initiated in these regions. Studies employed an electrode separation of 1.5 cm, corresponding to performing an ablation on tumors $\leq$1.0 cm. This raises an important question as to whether larger, more clinically relevant ablations can be performed with increased electrode separation, or whether treating larger tumors requires increasing the number of electrodes used. The H-FIRE ablation volume is confined by a marginal electric field threshold. The volume of tissue exposed to this electric field threshold can be increased by raising the applied voltage across electrodes or increasing the number of pulses. In terms of electrode configuration, increasing number of electrodes, electrode exposure, and electrode separation should all result in larger ablation volumes, provided the optimal settings characterized in this study are implemented and the voltage-separation ratio is not reduced.[24–26] Other possibilities for maximizing ablation volume using H-FIRE, such as the number of cycles or number of bursts, requires further study, but could result in thermal effects if not performed correctly.[24]

In addition to physical limitations, using multiple[2–6] electrode arrangements raises other clinical considerations. A notable disadvantage of current IRE technology is increased operative time and complexity associated with placing multiple electrodes, particularly if the tumor is located near a critical structure or deep within the parenchyma, and the need to do so using an open approach. Similarly, cost associated with performing IRE increases with intra-operative time and number of electrodes deployed. Thus, for H-FIRE to compete with existing ablation technology it must not only offer advantages over existing IRE, but advantages over thermal ablation.

A potential obstacle with existing IRE technology is the change in tissue impedance that can occur as a result of the IRE *per se*. That is, as cells within the electrical field undergo IRE, tissue conductivity changes and affects the flow of electrical current, and the presence of connective tissue and cell–cell interactions can further distort electric field distribution.[24] As a result, ablation geometries that differ from predicted models can arise.[16] By operating at higher frequencies, H-FIRE minimizes the effect of changing conductivities from electroporation and undermines electrical heterogeneities of surrounding tissue to dramatically increase ablation predictability.[25] In addition to the physical–electrical characteristics existing IRE requires long operative times compared to RFA/MWA due to the time required to place electrodes and the need to synchronize pulse delivery to cardiac electrical activity.[9,12,13] The use of H-FIRE does not overcome needle placement time. However, the electrical properties of H-FIRE should obviate the need for cardiac synchronization and reduce the time for pulse delivery.[15,16]

While H-FIRE appears to offer clear advantages over existing IRE, its role as an alternative to thermal ablation is more complex. Thermal ablation results in tissue desiccation and coagulative necrosis. While this is clearly the goal of RFA/MWA, it also limits use if tumors are located adjacent to critical structures, where collateral damage may have severe consequences. In this respect, H-FIRE may prove more amenable for use as a primary strategy to ablate tumors located in regions that cannot be thermally ablated or resected. Alternatively, H-FIRE could be used in conjunction with thermal ablation, whereby RFA/MWA is a primary ablative approach and H-FIRE is used at the tumor margin or in regions adjacent to critical structures. However, for either approach to be successful it is critical survival experiments be conducted to ascertain the long-term preservation of vascular and biliary architecture. As others report in large animal models, existing IRE can be used to create hepatic ablations $\leq$4 cm using dual electrodes[11] and 4–7 cm using 4 electrodes[26] while preserving vascular/biliary structures up to 2-weeks post-IRE. Similar studies are required for H-FIRE, and it will be of interest to determine whether performing H-FIRE near pedicles leads to longer term structural damage such as biliary stenosis.

Another consideration associated with thermal ablation and tissue desiccation is the effectiveness of adjuvant chemotherapy.[27] Increasing evidence exists that, at the edges of the IRE field, cells are exposed to reversible electroporation (RE).[28] In this instance cells may develop transient pore formation, but the

electrical stimulus is insufficient for defects to remain once the electrical field is removed.[29] The principle of RE has been extensively employed experimentally to introduce bioactive molecules that cannot otherwise cross the cell membrane.[30] The potential of RE at the margins of H-FIRE creates interesting possibilities for adjuvant chemotherapy, whereby uptake of cytotoxic agents in tumor cells is elevated by H-FIRE.

The absence of large animal models of hepatic cirrhosis and HCC mean studies were performed in healthy liver. Establishing the reproducibility of H-FIRE in heterogeneous tumor tissue, particularly in the setting of underlying cirrhosis, is of clear clinical relevance.[31] In addition to defining ablation characteristics and geometry in cirrhotic tissue, it would be of interest to characterize immune cell infiltration following ablation. Previous studies report the immune response is significantly less following RFA or laser-induced thermotherapy compared to cryotherapy, although still significant compared to resection.[32,33] In the current study immune cell infiltration appeared greater in the 300-pulse groups compared to the 100- or 200-pulse groups. Although these data were not quantified, it is tempting to speculate immune cell infiltration following 300-pulse H-FIRE delivery is an acute response to increased thermal necrosis compared to the 100- and 200-pulse groups. Potential complications associated H-FIRE in tumors arising in cirrhotic tissue, and the potential for immune cell infiltration in response to apoptotic bodies at longer post-ablation times, warrant further experimentation. These types of studies may be possible using freshly resected human cirrhotic-HCC tissue with an appropriate *ex vivo* design, or rodent models of HCC-cirrhosis with an adapted H-FIRE system.

In summary, data presented in this study demonstrate reproducible hepatic ablations using a bi-phasic high-frequency irreversible electroporation (H-FIRE) system in porcine liver *in vivo*. Unlike conventional IRE, H-FIRE did not require intraoperative paralytics or synchronization with cardiac activity, so simplifying the operative procedures and decreasing time. These data suggest H-FIRE may be more applicable where existing IRE is currently indicated, and an evolving option for select cases. However, for this technology to be considered in these instances it is necessary for additional experimentation to be performed, particularly with regard to limitations in ablation sizes, predictability in tumors arising in underlying disease states, and the longer term effects of H-FIRE on biliary and vascular architecture.

Acknowledgements

We wish to than Charity Patterson and Megan Templin (Dickson Advanced Analytics, Carolinas Medical Center, Charlotte, NC) for their help with statistical analysis.

Source of funding

Carolinas Healthcare Foundation (CHF), Virginia CIT (STTR15-002-LS).

Conflicts of interest

None declared.

References

1. Cho YK, Rhim H, Noh S. (2011) Radiofrequency ablation versus surgical resection as primary treatment of hepatocellular carcinoma meeting the Milan criteria: a systematic review. *J Gastroenterol Hepatol* 26: 1354–1360.
2. Lloyd DM, Lau KN, Welsh F, Lee KF, Sherlock DJ, Choti MA *et al*. (2011) International multicentre prospective study on microwave ablation of liver tumours: preliminary results. *HPB* 13:579–585.
3. Neimeyer DJSK, Iannitti DA, McKillop IH. (2014) Ablation therapy for hepatocellular carcinoma: past, present and future perspectives. *Hepat Oncol* 1:67–79.
4. Padma S, Martinie JB, Iannitti DA. (2009) Liver tumor ablation: percutaneous and open approaches. *J Surg Oncol* 100:619–634.
5. Poon RT, Ng KK, Lam CM, Ai V, Yuen J, Fan ST. (2004) Effectiveness of radiofrequency ablation for hepatocellular carcinomas larger than 3 cm in diameter. *Arch Surg* 139:281–287.
6. Swan RZ, Sindram D, Martinie JB, Iannitti DA. (2013) Operative microwave ablation for hepatocellular carcinoma: complications, recurrence, and long-term outcomes. *J Gastrointest Surg* 17:719–729.
7. Byrd JF, Agee N, McKillop IH, Sindram D, Martinie JB, Iannitti DA. (2011) Colour doppler ultrasonography provides real-time microwave field visualisation in an ex vivo porcine model. *HPB* 13:400–403.
8. Davalos RV, Mir IL, Rubinsky B. (2005) Tissue ablation with irreversible electroporation. *Ann Biomed Eng* 33:223–231.
9. Al-Sakere B, Andre F, Bernat C, Connault E, Opolon P, Davalos RV *et al*. (2007) Tumor ablation with irreversible electroporation. *PLoS One* 2: e1135.
10. Charpentier KP, Wolf F, Noble L, Winn B, Resnick M, Dupuy DE. (2011) Irreversible electroporation of the liver and liver hilum in swine. *HPB* 13: 168–173.
11. Chen X, Ren Z, Zhu T, Zhang X, Peng Z, Xie H *et al*. (2015) Electric ablation with irreversible electroporation (IRE) in vital hepatic structures and follow-up investigation. *Sci Rep* 5:16233.
12. Charpentier KP. (2012) Irreversible electroporation for the ablation of liver tumors: are we there yet? *Arch Surg* 147:1053–1061.
13. Martin, RC, 2nd, Kwon D, Chalikonda S, Sellers M, Kotz E, Scoggins C *et al*. (2015) Treatment of 200 locally advanced (stage III) pancreatic adenocarcinoma patients with irreversible electroporation: safety and efficacy. *Ann Surg* 262:486–494. discussion 92–4.
14. Simo KA, Tsirline VB, Sindram D, McMillan MT, Thompson KJ, Swan RZ *et al*. (2013) Microwave ablation using 915-MHz and 2.45-GHz systems: what are the differences? *HPB* 15:991–996.
15. Arena CB, Sano MB, Rossmeisl, JH, Jr., Caldwell JL, Garcia PA, Rylander MN *et al*. (2011) High-frequency irreversible electroporation (H-FIRE) for non-thermal ablation without muscle contraction. *Biomed Eng Online* 10:102.
16. Arena CB, Sano MB, Rylander MN, Davalos RV. (2011) Theoretical considerations of tissue electroporation with high-frequency bipolar pulses. *IEEE Trans Biomed Eng* 58:1474–1482.
17. Rossmeisl, JH, Jr., Garcia PA, Pancotto TE, Robertson JL, Henao-Guerrero N, Neal, RE, 2nd *et al*. (2015) Safety and feasibility of the NanoKnife system for irreversible electroporation ablative treatment of canine spontaneous intracranial gliomas. *J Neurosurg* 123:1008–1025.

18. Au JT, Kingham TP, Jun K, Haddad D, Gholami S, Mojica K *et al*. (2013) Irreversible electroporation ablation of the liver can be detected with ultrasound B-mode and elastography. *Surgery* 153:787–793.
19. Swet JH, Pacheco HJ, Iannitti DA, El-Ghanam A, McKillop IH. (2014) A silica-calcium-phosphate nanocomposite drug delivery system for the treatment of hepatocellular carcinoma: in vivo study. *J Biomed Mater Res B Appl Biomater* 102:190–202.
20. Stadlbauer V, Lang-Olip I, Leber B, Mayrhauser U, Koestenbauer S, Tawdrous M *et al*. (2016) Immunohistochemical and radiological characterization of wound healing in porcine liver after radiofrequency ablation. *Histol Histopathol* 31:115–129.
21. Sugimoto K, Moriyasu F, Kobayashi Y, Kasuya K, Nagakawa Y, Tsuchida A *et al*. (2015) Assessment of various types of US findings after irreversible electroporation in porcine liver: comparison with radiofrequency ablation. *J Vasc Interv Radiol* 26, 279–287.e3.
22. Facciorusso A, Di Maso M, Muscatiello N. (2016) Microwave ablation versus radiofrequency ablation for the treatment of hepatocellular carcinoma: a systematic review and meta-analysis. *Int J Hyperthermia*, 1–6.
23. Seshadri RM, Baker EH, Templin M, Swan RZ, Martinie JB, Vrochides D *et al*. (2015) Outcomes of surgical resection and loco-regional therapy in patients with stage 3A hepatocellular carcinoma: a retrospective review from the national cancer database. *HPB* 17:964–968.
24. Neal, RE, 2nd, Garcia PA, Robertson JL, Davalos RV. (2011) Experimental characterization of intrapulse tissue conductivity changes for electroporation. *Conf Proc IEEE Eng Med Biol Soc* 2011:5581–5584.
25. Sano MB, Arena CB, Bittleman KR, DeWitt MR, Cho HJ, Szot CS *et al*. (2015) Bursts of bipolar microsecond pulses inhibit tumor growth. *Sci Rep* 5:14999.
26. Appelbaum L, Ben-David E, Faroja M, Nissenbaum Y, Sosna J, Goldberg SN. (2014) Irreversible electroporation ablation: creation of large-volume ablation zones in in vivo porcine liver with four-electrode arrays. *Radiology* 270:416–424.
27. Vollherbst D, Bertheau RC, Fritz S, Mogler C, Kauczor HU, Ryschich E *et al*. (2016) Electrochemical effects after transarterial chemoembolization in combination with percutaneous irreversible electroporation: observations in an acute porcine liver model. *J Vasc Interv Radiol* 27:913–921.
28. Golberg A, Bruinsma BG, Uygun BE, Yarmush ML. (2015) Tissue heterogeneity in structure and conductivity contribute to cell survival during irreversible electroporation ablation by “electric field sinks”. *Sci Rep* 5: 8485.
29. Turjanski P, Olaiz N, Maglietti F, Michinski S, Suarez C, Molina FV *et al*. (2011) The role of pH fronts in reversible electroporation. *PLoS One* 6: e17303.
30. Joergensen M, Agerholm-Larsen B, Nielsen PE, Gehl J. (2011) Efficiency of cellular delivery of antisense peptide nucleic acid by electroporation depends on charge and electroporation geometry. *Oligonucleotides* 21:29–37.
31. Fattovich G, Stroffolini T, Zagni I, Donato F. (2004) Hepatocellular carcinoma in cirrhosis: incidence and risk factors. *Gastroenterology* 127(5 Suppl. 1):S35–S50.
32. Ng KK, Lam CM, Poon RT, Shek TW, To JY, Wo YH *et al*. (2004) Comparison of systemic responses of radiofrequency ablation, cryotherapy, and surgical resection in a porcine liver model. *Ann Surg Oncol* 11:650–657.
33. Jansen MC, van Hillegersberg R, Schoots IG, Levi M, Beek JF, Crezee H *et al*. (2010) Cryoablation induces greater inflammatory and coagulative responses than radiofrequency ablation or laser induced thermotherapy in a rat liver model. *Surgery* 147:686–695.